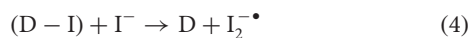# High-efficiency dye-sensitized solar cells with ferrocene-based electrolytes

Torben Daeneke[1†], Tae-Hyuk Kwon[2†], Andrew B. Holmes[2], Noel W. Duffy[3], Udo Bach[1,4]★ and Leone Spiccia[1]★

Dye-sensitized solar cells based on iodide/triiodide (I^-/I_3^-) electrolytes are viable low-cost alternatives to conventional silicon solar cells. However, as well as providing record efficiencies of up to 12.0%, the use of I^-/I_3^- in such solar cells also brings about certain limitations that stem from its corrosive nature and complex two-electron redox chemistry. Alternative redox mediators have been investigated, but these generally fall well short of matching the performance of conventional I^-/I_3^- electrolytes. Here, we report energy conversion efficiencies of 7.5% (simulated sunlight, AM1.5, 1,000 W m^{-2}) for dye-sensitized solar cells combining the archetypal ferrocene/ferrocenium (Fc/Fc^+) single-electron redox couple with a novel metal-free organic donor–acceptor sensitizer (Carbz-PAHTDTT). These Fc/Fc^+-based devices exceed the efficiency achieved for devices prepared using I^-/I_3^- electrolytes under comparable conditions, revealing the great potential of ferrocene-based electrolytes in future dye-sensitized solar cells applications. This improvement results from a more favourable matching of the redox potential of the ferrocene couple with that of the new donor–acceptor sensitizer.
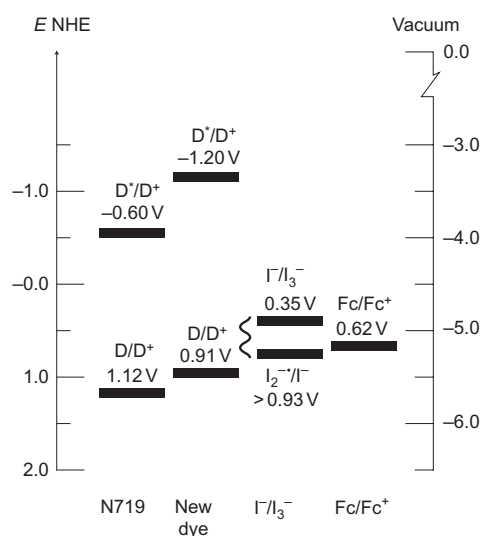
L
ight harvesting in dye-sensitized solar cells (DSCs) is accomplished by a self-assembled monolayer of dye molecules, located at the interface of a mesoporous wide-bandgap semiconductor electrode and an electrolyte[1]. The electrolyte fulfils two major functions. First, a redox mediator is present that effectively regenerates the dye following a photoinduced charge injection from the dye into the semiconductor electrode (see equations (1) to (5)). Second, it facilitates charge transport to the adjacent counter-electrode, typically through an ion diffusion mechanism. The iodide/triiodide (I^-/I_3^-) couple is by far the most common redox couple used in DSC electrolytes, affording unrivalled energy conversion efficiencies of up to 12.0% and 10.3% for ruthenium-based sensitizers and metal-free organic sensitizers, respectively[2–4]. Despite its superior performance, the I^-/I_3^- couple does have some limitations that derive from its corrosive nature and complex redox chemistry[5]. Overcoming these constraints could lead to further improvements in DSC performance and ease of fabrication.

The following equations summarize the electron transfer reactions involved in photocurrent generation in a conventional DSC (I-DSC) based on the two-electron I^-/I_3^- redox system:
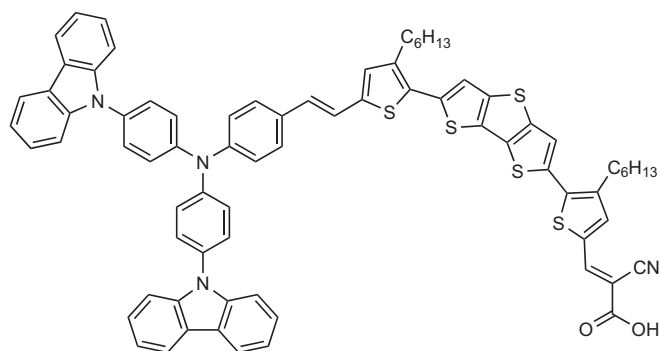
$$D + h\nu \rightarrow D^* \tag{1}$$

$$D^* \rightarrow e^-(TiO_2) + D^+ \tag{2}$$

$$D^+ + I^- \rightarrow (D-I) \tag{3}$$

$$(D-I) + I^- \rightarrow D + I_2^{-\bullet} \tag{4}$$

$$2I_2^{-\bullet} \rightarrow I_3^- + I^- \tag{5}$$

Dye regeneration involves the formation of the intermediate radical species $I_2^{-\bullet}$, which exhibits a more negative redox potential than the corresponding standard redox potential of I^-/I_3^- (Fig. 1), thus

representing an additional energy activation barrier for the dye regeneration process[5]. For DSCs based on the record-performing ruthenium-based sensitizers, such as N719 (di-tetrabutylammonium-*cis-bis*(isothiocyanato)*bis*(2,2′-bipyridyl-4,4′-dicarboxylato) ruthenium(II)), the difference between the redox potential of the dye, $E(D/D^+)$ (1.0–1.1 V), and the I/I_3^- redox couple, $E(I^-/I_3^-)$ (E^0 ranges from 0.35 V in acetonitrile[5] to typically 0.4 V for electrolytes optimized for ruthenium sensitizer-based DSCs[6]), is in excess of 600 mV. For photons with an energy of 2 eV, this means that more than 30% of the original photon
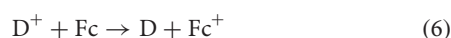

Figure 1 | Energy levels of DSC components, approximate redox potentials and band energies of the different components. Data for N719, Carbz-PAHTDTT (new dye), I^-/I_3^-, and Fc/Fc^+ versus normal hydrogen electrode (NHE)[5,21,37].

[1]School of Chemistry and ARC Centre of Excellence for Electromaterials Science, Monash University, Victoria 3800, Australia, [2]School of Chemistry, Bio21 Institute, University of Melbourne, Victoria 3010, Australia, [3]CSIRO Energy Technology, Clayton, VIC 3169, Australia, [4]Department of Materials Engineering, Monash University, Victoria 3800, Australia; [†]These authors contributed equally to this work. *e-mail: leone.spiccia@monash.edu; udo.bach@monash.edu

211

Figure 2 | Structure of the organic sensitizer Carbz-PAHTDTT.

energy drives the dye regeneration process. By replacing I^-/I_3^- with a single-electron transfer mediator,

$$D^+ + Fc \rightarrow D + Fc^+ \qquad (6)$$

it should be feasible to reduce the redox potential difference between dye and electrolyte, affording significant improvements in DSC efficiency.

While imposing additional activation barriers for dye regeneration, the complex redox mechanism of I^-/I_3^- is also considered to be crucially beneficial for the inhibition of interfacial charge recombination in DSCs (for example, involving reaction of the injected electron with the triodide ion present in the electrolyte), thus affording high conversion efficiencies[7,8]. The challenge in the development of alternative redox mediators is to ensure that potential efficiency gains afforded by lowering the driving force for dye regeneration are not compromised by efficiency losses resulting from increased interfacial charge recombination rates.

Previous attempts to replace the I_3^-/I^- couple have been summarized well in recent reviews[9–11]. Most noticeable are a range of cobalt complexes that perform well under low light conditions but suffer from poor charge transport, limiting the efficiency to 4% under standard solar irradiation (AM1.5, 1,000 W m^{-2})[12]. However, Feldt and colleagues have recently reported an efficiency of 6.7% for a cobalt polypyridine redox mediator[13]. Copper[14] and nickel[15] complexes have also been examined, but led to DSC efficiencies below 2% at full simulated sunlight. Electrolytes based on the Br_3^-/Br^- redox system have been used in DSCs, and have achieved conversion efficiencies of up to 5.2%, but, unfortunately, these exhibit corrosive properties that are comparable to those of the conventional I_3^-/I^- electrolyte[16]. DSCs constructed with organic redox couples, such as TEMPO (2,2,6,6-tetramethylpiperidine-1-oxyl) and *tris*-[4-(2-methoxy-ethoxy)-phenyl]-amine[17] have yielded efficiencies of 5.4% (ref. 5) and 2.4%, respectively. Recently, Wang and colleagues have reported a new disulfide/thiolate redox couple featuring a two-electron redox process that achieved an efficiency of 6.4% under 1,000 W m^{-2} simulated sunlight[18]. Alternative approaches are being developed that aim to replace the redox electrolytes in DSCs with solid-state charge transport materials. For example, efficiencies of up to 5.1% have been reported for DSCs constructed with CuI (ref. 19) and spiro-OMeTAD[20].

An excellent choice for an alternative redox couple is the archetypal ferrocene/ferrocenium hexafluorophosphate (Fc/Fc^+) couple. This non-corrosive mediator exhibits well-defined electrochemistry (it is an IUPAC-recommended reference redox couple), is commercially available on a large scale and has a more favourable redox potential than the I_3^-/I^- redox couple (0.62 V cf. 0.35 V vs. NHE)[5,21], which should result in a higher open-circuit voltage (V_{OC}) (Fig. 1). Dye regeneration by ferrocene is a simple one-electron transfer reaction that does not involve the cleavage or
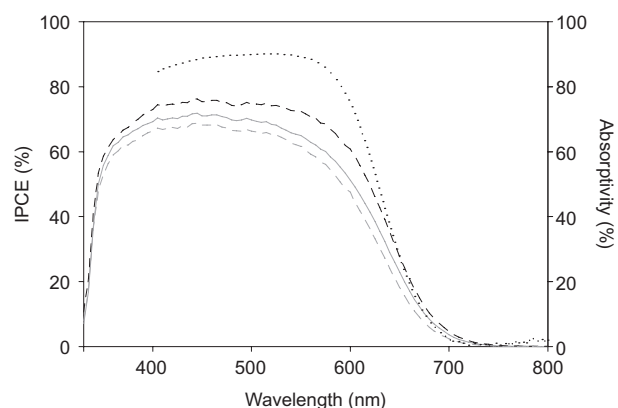
reformation of chemical bonds or the formation of high-energy intermediate radical species (equations (4) and (5)). Furthermore, a plethora of substituted ferrocene compounds are known, with hundreds being commercially available. Thus, the ferrocene redox potential can be fine-tuned easily through the introduction of specific substituents on the cyclopentadienyl ring[22,23]. These promising features have led to attempts to use ferrocene as a redox mediator in DSCs, but the resulting devices exhibited low efficiencies ($\eta < 0.4\%$)[8,24–26].
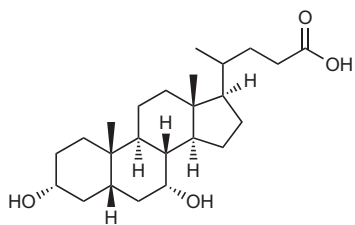
Results and discussion

In this study, we have explored the potential use of Fc/Fc^+ electrolytes as model systems for the construction of high-efficiency DSCs based on single-electron transfer redox mediators. The exclusion of oxygen during electrolyte preparation and cell construction was of paramount importance in achieving improved and reproducible device performances, due to the inherent instability of ferrocenium in the presence of molecular oxygen[8,27,28].

A novel metal-free organic dye (Carbz-PAHTDTT, Fig. 2; for synthesis and characterization see Supplementary Information) was used for this study. Carbz-PAHTDTT affords excellent light-harvesting properties when used in conjunction with thin TiO_2 electrodes comprising a 2.2 μm mesoporous TiO_2 layer (particle size, 18 nm) and a 4.4 μm TiO_2 scattering layer (particle size, 400 nm). Typical dye absorptivity data for these electrodes are shown in Fig. 3. Thinner than usual TiO_2 electrodes were used in anticipation of accelerated recombination phenomena in Fc-DSCs. The combination of thin TiO_2 electrodes and organic dyes with high extinction coefficients has previously been proven to be beneficial for solid-state DSCs based on organic charge transport materials, where accelerated charge recombination is of equal concern[29].
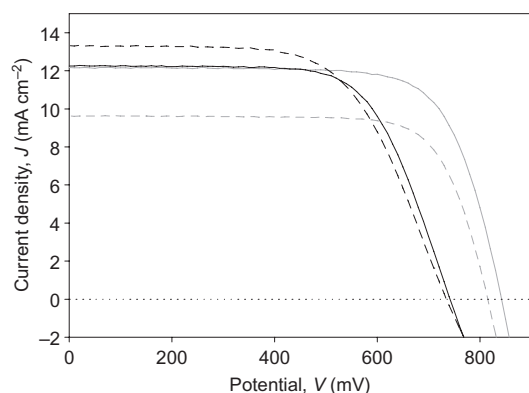
Fc-DSCs were assembled with electrolytes containing ferrocene (Fc), ferrocenium hexafluorophosphate ($FcPF_6$) and *tert*-butylpyridine (*t*-BP) in acetonitrile. Increases in efficiency were found to result from the addition of *t*-BP. These are typically explained in terms of reduced charge recombination due to the passivation of TiO_2 surface states through interaction with *t*-BP[30]. The previously reported rapid decomposition of the ferrocenium ion in the presence of *t*-BP (ref. 22) was not observed, which is in accordance with the known electrochemistry of ferrocene in pyridine[31,32]. Adsorption of Carbz-PAHTDTT onto TiO_2 was routinely performed in the presence of chenodeoxycholic acid (cheno) (Fig. 4) as co-adsorbent, as this consistently led to improved DSC

Figure 3 | IPCE results and absorptivity of the Carbz-PAHTDTT sensitized TiO₂ film. Black dashed line, I-DSC; grey solid line, Fc-DSC-C; grey dashed line, Fc-DSC. Black dotted line indicates the absorptivity of the sensitized TiO₂ film. IPCE spectra are recorded at low light conditions (<2% sun). Electrolyte composition is summarized in Supplementary Table S1. Double-layer TiO₂ films (2.2 μm mesoporous TiO₂ (18 nm) + 4.4 μm scattering TiO₂ (400 nm)) were used for constructing all DSCs.

Figure 4 | Structure of the co-adsorbent and electrolyte additive chenodeoxycholic acid (cheno).

Figure 5 | Photocurrent density–voltage curves at simulated one sun (1,000 W m⁻²) irradiation (AM1.5). Comparison of DSC performance for optimized devices: sensitized with Carbz-PAHTDTT, based on iodine/iodide electrolytes in acetonitrile/valeronitrile (black line), or the Fc/Fc$^+$ electrolyte in acetonitrile (grey), with cheno (solid, I-DSC-C and Fc-DSC-C) and without cheno (dashed, I-DSC and Fc-DSC). Electrolyte composition is summarized in Supplementary Table S1. Double-layer TiO$_2$ films (2.2 µm mesoporous TiO$_2$ (18 nm) + 4.4 µm scattering TiO$_2$ (400 nm)) were used for the construction of all DSCs.

performances for all the electrolyte systems studied. This is in agreement with previous studies applying metal-free organic dyes, and is typically explained in terms of a reduction in dye aggregation and improved surface passivation[33]. In this study, we have also investigated the effect of cheno as an electrolyte additive on DSC performance (I-DSC-C and Fc-DSC-C).

The incident photon-to-electron conversion efficiency (IPCE) spectra of Carbz-PAHTDTT-sensitized solar cells with optimized Fc/Fc$^+$ and I$^-$/I$_3^-$ electrolyte compositions are shown in Fig. 3. These spectra provide quantification of the efficiency (plotted as a percentage versus wavelength (energy) of incident photons) of conversion of absorbed photons into electrons (current). The IPCE spectrum of the Fc-DSC closely matches that of the I-DSC and both closely follow the shape of the absorptivity of the sensitized TiO$_2$ layer. The addition of cheno had no effect on the IPCE of the I$^-$/I$_3^-$ devices (I-DSC-C not shown). In contrast, significant improvements were observed when cheno was added to the ferrocene electrolyte. The maximum IPCE achieved by the Fc-DSC-C is 72%. The absorptivity exceeding 80% at wavelengths up to 600 nm illustrates the excellent light-harvesting properties of the Carbz-PAHTDTT-sensitized TiO$_2$ films.
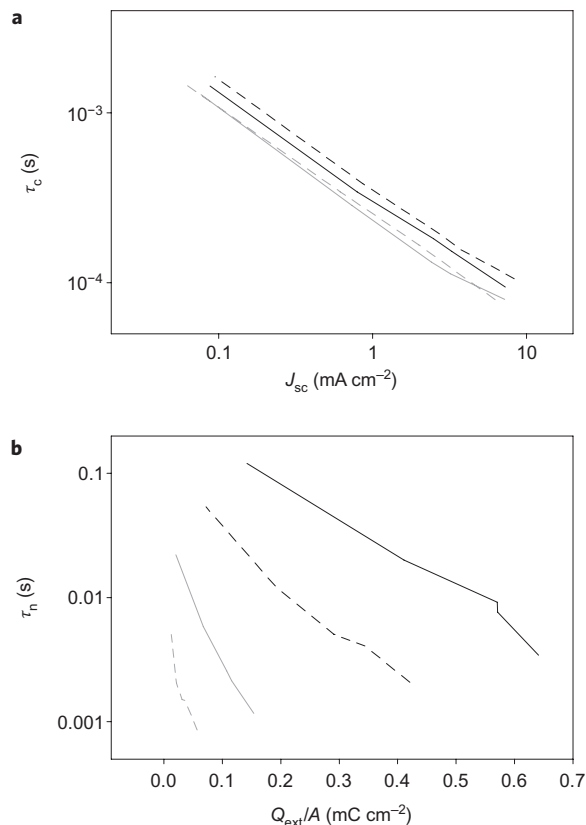
The current/voltage characteristics under simulated one sun solar illumination (AM1.5; 1,000 W m⁻²) of Fc-DSCs and I-DSCs are presented in Fig. 5 and Table 1. Fc-DSCs, in combination with the donor–acceptor sensitizer Carbz-PAHTDTT, show a remarkable performance improvement with the addition of cheno to the electrolyte, leading to an increase in short-circuit current density (J_{SC}) and open-circuit voltage (V_{OC}) that result in an overall energy conversion efficiency of 7.5%. To our knowledge,

Table 1 | Tabulated photovoltaic performance data of the DSC in Fig. 5, measured at one sun simulated sunlight (AM1.5).

	J_{OC} (mA cm⁻²)	V_{OC} (mV)	FF (%)	η (%)
I-DSC	13.3	735	62	6.1
I-DSC-C	12.3	742	67	6.1
Fc-DSC	9.6	815	75	5.9
Fc-DSC-C	12.2	842	73	7.5

this is the highest efficiency that has ever been reported at one sun for a DSC that uses a non-I$^-$/I$_3^-$ electrolyte. It is 20 times higher than previously reported values for Fc-DSCs[24]. In our experiment, an efficiency of 0.33% was measured when the ferrocene electrolyte was used in DCSs in conjunction with the standard N719 ruthenium dye (see Supplementary Information). In comparison, addition of cheno to the I-DSC resulted in a decrease in J_{SC}, coupled with an increase in V_{OC} and fill factor (FF), which left the overall efficiency unchanged at 6.1–6.2%. The Fc-DSC clearly outperformed the classical I-DSC. This remarkable conversion efficiency is mainly a consequence of the high photovoltage of 842 mV achieved for the Fc-DSC, which exceeds the V_{OC} of the I-DSC by 100 mV.

These results show that we can successfully translate the more favourable Fc/Fc$^+$ redox potential (Fig. 1) into an overall efficiency increase. Carbz-PAHTDTT sensitized I-DSCs based on thicker TiO$_2$ films (12 µm + 6 µm scattering) yielded maximum energy conversion efficiencies of 6.3%. For comparison, DSCs assembled

Figure 6 | IMVS and IMPS spectroscopy. a, Mean charge transit time versus short-circuit current. **b,** Electron lifetime versus extracted charge for Carbz-PAHTDTT-sensitized DSCs. Fc-DSC (grey dashed line), Fc-DSC-C (grey solid line), I-DSC (black dashed line) and I-DSC-C (black solid line). Double-layer TiO$_2$ films (2.2 µm mesoporous TiO$_2$ (18 nm) + 4.4 µm scattering TiO$_2$ (400 nm)) were used for the construction of all DSCs.

with a standard high-efficiency ruthenium sensitizer, N719 (ref. 34), and high-performance I^-/I_3^- electrolytes yielded 6.8% efficiency for thin TiO_2 layers (2.2 μm + 4.4 μm scattering) and 8.2% efficiency for thick TiO_2 layers (12 μm + 6 μm scattering; see Supplementary Table S2).

Intensity-modulated photovoltage and photocurrent spectroscopy (IMVS and IMPS)[35], complemented by charge extraction experiments, were used to determine the electron lifetime and mean transit time of photoinjected charge carriers. Figure 6a presents the IMPS results, indicating that similar mean electron transit times were observed for both redox systems in the absence and presence of cheno in the electrolyte. Charge extraction measurements according to Duffy and colleagues[36] were used to determine the amount of charge stored in DSCs as a function of V_{OC} (Supplementary Fig. S1). The results obtained from the IMVS measurements, carried out to determine the electron lifetime of photoinjected charge carriers under V_{OC} conditions, and charge extraction experiments have been combined to give the electron lifetime as a function of charge stored in the DSC (Fig. 6b). The results confirm that charge recombination is more rapid in Fc-DSCs than in I-DSCs. The addition of cheno significantly increases the electron lifetime for both redox systems, presumably by blocking interfacial charge recombination. It can be postulated that the cheno present in the electrolyte helps to form a hermetic protection through the establishment of a steady-state equilibrium between surface-adsorbed and electrolyte-borne molecules. The origin of the beneficial effects of cheno is the subject of ongoing studies.

Conclusion

In this study, we have demonstrated that the IUPAC-recommended Fc/Fc^+ reference redox couple can be used to construct highly efficient DSCs that exceed the performance of DSCs using the corrosive and mechanistically more complex I^-/I_3^- couple as redox mediator. Exclusion of oxygen from the DSC construction process together with optimization of the TiO_2 film structure and electrolyte composition yielded energy conversion efficiencies of up to 7.5% when the Fc/Fc^+ redox mediator was used in conjunction with the novel metal-free organic sensitizer Carbz-PAHTDTT. The increase in energy conversion by a factor of almost 20 over previously reported values[24] reveals the great potential of ferrocene-based electrolytes for future applications in DSCs. A net V_{OC} increase of 100 mV could be realized, due to the more favourable position of the electrochemical redox potential of ferrocene, compared to iodide. Generally, the redox potential of ferrocene compounds can be easily tuned through functionalization of the cyclopentadienyl rings with a variety of substituents. This offers the opportunity to carefully match the dye-regeneration driving forces, which in turn could result in further significant increases in V_{OC} and therefore cell performance[22,23]. Work on this aspect is in progress.

Methods

DSCs were constructed using common construction techniques (see Supplementary Information). IMVS and IMPS spectroscopy and charge extraction measurements were performed as described elsewhere[35,36]. The dye Carbz-PAHTDTT was synthesized as described in the Supplementary Information.

References

1. O'Regan, B. & Grätzel, M. A low-cost, high-efficiency solar cell based on dye-sensitized colloidal TiO_2 films. *Nature* **353**, 737–740 (1991).
2. Chen, C.-Y. *et al.* Highly efficient light-harvesting ruthenium sensitizer for thin-film dye-sensitized solar cells. *ACS Nano* **3**, 3103–3109 (2009).
3. Zeng, W. *et al.* Efficient dye-sensitized solar cells with an organic photosensitizer featuring orderly conjugated ethylenedioxythiophene and dithienosilole blocks. *Chem. Mater.* **22**, 1915–1925 (2010).
4. Yu, Q. *et al.* High-efficiency dye-sensitized solar cells: The influence of lithium ions on exciton dissociation, charge recombination, and surface states. *ACS Nano* **4**, 6032–6038 (2010).
5. Boschloo, G. & Hagfeldt, A. Characteristics of the iodide/triiodide redox mediator in dye-sensitized solar cells. *Acc. Chem. Res.* **42**, 1819–1826 (2009).
6. Zhang, Z., Chen, P., Murakami, T. N., Zakeeruddin, S. M. & Grätzel, M. The 2,2,6,6-tetramethyl-1-piperidinyloxy radical: an efficient, iodine-free redox mediator for dye-sensitized solar cells. *Adv. Funct. Mater.* **18**, 341–346 (2008).
7. Schlichthoerl, G., Huang, S. Y., Sprague, J. & Frank, A. J. Band edge movement and recombination kinetics in dye-sensitized nanocrystalline TiO_2 solar cells: a study by intensity modulated photovoltage spectroscopy. *J. Phys. Chem. B* **101**, 8141–8155 (1997).
8. Gregg, B. A., Pichot, F., Ferrere, S. & Fields, C. L. Interfacial recombination processes in dye-sensitized solar cells and methods to passivate the interfaces. *Phys. Chem. B* **105**, 1422–1429 (2001).
9. Ardo, S. & Meyer, G. J. Photodriven heterogeneous charge transfer with transition-metal compounds anchored to TiO_2 semiconductor surfaces. *Chem. Soc. Rev.* **38**, 115–164 (2009).
10. Hagfeldt, A., Boschloo, G., Sun, L., Kloo, L. & Pettersson, H. Dye-sensitized solar cells. *Chem. Rev.* **110**, 6595–6663 (2010).
11. Yanagida, S., Yu, Y. & Manseki, K. Iodine/iodide-free dye-sensitized solar cells. *Acc. Chem. Res.* **42**, 1827–1838 (2009).
12. Nusbaumer, H., Moser, J.-E., Zakeeruddin, S. M., Nazeeruddin, M. K. & Grätzel, M. $Co^{II}(dbbip)_2^{2+}$ complex rivals tri-iodide/iodide redox mediator in dye-sensitized photovoltaic cells. *J. Phys. Chem. B* **105**, 10461–10464 (2001).
13. Feldt, S. M. *et al.* Design of organic dyes and cobalt polypyridine redox mediators for high-efficiency dye-sensitized solar cells. *J. Am. Chem. Soc.* **132**, 16714–16724 (2010).
14. Hattori, S., Wada, Y., Yanagida, S. & Fukuzumi, S. Blue copper model complexes with distorted tetragonal geometry acting as effective electron-transfer mediators in dye-sensitized solar cells. *J. Am. Chem. Soc.* **127**, 9648–9654 (2005).
15. Li, T. C. *et al.* Ni(III)/(IV) *Bis*(dicarbollide) as a fast, noncorrosive redox shuttle for dye-sensitized solar cells. *J. Am. Chem. Soc.* **132**, 4580–4582 (2010).
16. Teng, C. *et al.* Two novel carbazole dyes for dye-sensitized solar cells with open-circuit voltages up to 1 V based on Br^-/Br_3^- electrolytes. *Org. Lett.* **11**, 5542–5545 (2009).
17. Snaith, H. J., Zakeeruddin, S. M., Wang, Q., Pechy, P. & Grätzel, M. Dye-sensitized solar cells incorporating a 'liquid' hole-transporting material. *Nano Lett.* **6**, 2000–2003 (2006).
18. Wang, M. *et al.* An organic redox electrolyte to rival triiodide/iodide in dye-sensitized solar cells. *Nat. Chem.* **2**, 385–389 (2010).
19. Tennakone, K. *et al.* A solid-state photovoltaic cell sensitized with a ruthenium bipyridyl complex. *J. Phys. D* **31**, 1492–1496 (1998).
20. Yum, J. H., Chen, P., Grätzel, M. & Nazeeruddin, M. Recent developments in solid-state dye-sensitized solar cells. *ChemSusChem* **1**, 699–707 (2008).
21. Pavlishchuk, V. V. & Addison, A. W. Conversion constants for redox potentials measured versus different reference electrodes in acetonitrile solutions at 25 °C. *Inorg. Chim. Acta* **298**, 97–102 (2000).
22. Brown, K. N. *et al.* Electrochemistry of chlorinated ferrocenes: stability of chlorinated ferrocenium ions. *Dalton Trans.* 835–840 (1993).
23. Noviandri, I. *et al.* The decamethylferrocenium/decamethylferrocene redox couple: a superior redox standard to the ferrocenium/ferrocene redox couple for studying solvent effects on the thermodynamics of electron transfer. *J. Phys. Chem. B* **103**, 6713–6722 (1999).
24. Hamann, T. W., Farha, O. K. & Hupp, J. T. Outer-sphere redox couples as shuttles in dye-sensitized solar cells. Performance enhancement based on photoelectrode modification via atomic layer deposition. *J. Phys. Chem. C* **112**, 19756–19764 (2008).
25. Waita, S. M. *et al.* Electrochemical characterization of TiO_2 blocking layers prepared by reactive DC magnetron sputtering. *J. Electroanal. Chem.* **637**, 79–83 (2009).
26. Feldt, S. M., Cappel, U. B., Johansson, E. M. J., Boschloo, G. & Hagfeldt, A. Characterization of surface passivation by poly(methylsiloxane) for dye-sensitized solar cells employing the ferrocene redox couple. *J. Phys. Chem. C* **114**, 10551–10558 (2010).
27. Zotti, G., Schiavon, G., Zecchin, S. & Favretto, D. Dioxygen-decomposition of ferrocenium molecules in acetonitrile: the nature of the electrode-fouling films during ferrocene electrochemistry. *J. Electroanal. Chem.* **456**, 217–221 (1998).
28. Hurvois, J. P. & Moinet, C. Reactivity of ferrocenium cations with molecular oxygen in polar organic solvents: decomposition, redox reactions and stabilization. *J. Organomet. Chem.* **690**, 1829–1839 (2005).
29. Schmidt-Mende, L. *et al.* Organic dye for highly efficient solid-state dye-sensitized solar cells. *Adv. Mater.* **17**, 813–815 (2005).

30. Huang, S. Y., Schlichthörl, G., Nozik, A. J., Grätzel, M. & Frank, A. J. Charge recombination in dye-sensitized nanocrystalline TiO$_2$ solar cells. *J. Phys. Chem. B* **101,** 2576–2582 (1997).

31. Turbanov, K. Y. Interaction of ferricinium cation with pyridine. *Zhurnal Obshchei Khimii* **63,** 1803–1809 (1993).

32. Mukherjee, L. M. Standard potential of the ferrocene–ferricinium electrode in pyridine. Evaluation of proton medium effect. *J. Phys. Chem. B* **76,** 243–245 (1972).

33. Wang, Z.-S. *et al.* Thiophene-functionalized coumarin dye for efficient dye-sensitized solar cells: electron lifetime improved by coadsorption of deoxycholic acid. *J. Phys. Chem. C* **111,** 7224–7230 (2007).

34. Nazeeruddin, M. K. *et al.* Combined experimental and DFT-TDDFT computational study of photoelectrochemical cell ruthenium sensitizers. *J. Am. Chem. Soc.* **127,** 16835–16847 (2005).

35. Fisher, A. C., Peter, L. M., Ponomarev, E. A., Walker, A. B. & Wijayantha, K. G. U. Intensity dependence of the back reaction and transport of electrons in dye-sensitized nanocrystalline TiO$_2$ solar cells. *J. Phys. Chem. B* **104,** 949–958 (2000).

36. Duffy, N. W., Peter, L. M., Rajapakse, R. M. G. & Wijayantha, K. G. U. A novel charge extraction method for the study of electron transport and interfacial transfer in dye sensitised nanocrystalline solar cells. *Electrochem. Commun.* **2,** 658–662 (2000).

37. Bessho, T. *et al.* New paradigm in molecular engineering of sensitizers for solar cell applications. *J. Am. Chem. Soc.* **131,** 5930–5934 (2009).

Author contributions

L.S., U.B. and A.B.H. proposed the research. T.D. designed the electrolyte, developed the construction technique, fabricated the DSCs and carried out device characterization. T.-H.K. designed, synthesized and characterized the dye. N.W.D. and T.D. carried out the charge extraction and IMVS–IMPS measurements on instruments designed by N.W.D. L.S., U.B. and T.D. were mainly responsible for writing the manuscript, with contributions from N.W.D., T.-H.K. and A.B.H.

Additional information

The authors declare no competing financial interests. Supplementary information accompanies this paper at www.nature.com/naturechemistry. Reprints and permission information is available online at http://npg.nature.com/reprintsandpermissions/. Correspondence and requests for materials should be addressed to U.B. and L.S.